Modern Journal of Statistics
2(2), 174–200
DOI: https://doi.org/10.64389/mjs.2026.02244
https://sphinxsp.org/journal/index.php/mjs/

Research article

A New Modification for the Inverse Rayleigh Distribution with Properties, Entropy Information, and Applications to Environmental Data

I. Elbatal[1], **Ehab M. Almetwally**[1], **Meraou M. A.**[2,*], **Samirah Alzubaidi**[3], **M. H. Harpy**[4], **Elkhateeb S Aly**[5], **Rahmtalla Y. Yagoub**[6], **Abdisalan Ahmed Osman**[7]

[1]Department of Mathematics and Statistics, Faculty of Science, Imam Mohammad Ibn Saud Islamic University (IMSIU), Riyadh 11432, Saudi Arabia; iielbatal@imamu.edu.sa; emalmetwally@imamu.edu.sa

[2]Laboratory of Statistics and Stochastic Processes, University of Djillali Liabes, BP 89, Sidi Bel Abbes 22000, Algeria; amine.meraou@univ-sba.dz

[3]Department of Mathematics, Al-Qunfudah University College, Umm Al-Qura University, Mecca, Saudi Arabia; shzubaidi@uqu.edu.sa

[4]Department of Mathematics, Faculty of Science, Suez Canal University, Ismailia 41522, Egypt; mahmoud_haussieny@science.suez.edu.eg

[5]Department of Mathematics, College of Science, Jazan University, P.O. Box 114, Jazan 45142, Kingdom of Saudi Arabia; elkhateeb@jazanu.edu.sa

[6]Department of Statistics, Faculty of Science, University of Tabuk, Tabuk 71491, Kingdom of Saudi Arabia; ryaaqoub@ut.edu.sa

[7]Department of Statistics, College of Natural and Computational science, University of Kabridahar, Somali Regional State, Kebri Dehar, Ethiopia; abdisalan.ahmed18@uok.edu.et

* **Correspondence:** amine.meraou@univ-sba.dz

ARTICLE INFO

Keywords:
Rayleigh distribution
Application
Entropy measures
Environmental studies
Simulation

Mathematics Subject Classification:
62H05, 60E05, 62P12, 65C20

Important Dates:
Received: 3 November 2025
Revised: 18 June 2026
Accepted: 30 June 2026
Online: 5 July 2026

ABSTRACT

In the present study, we develop a new version of the inverse Rayleigh model using the odd-type G family of distributions. The proposed model is highly flexible and exhibits various behaviors in terms of its density and hazard functions. We study the mathematical properties of this new model, such as moments, quantile function, moment generating function, skewness, kurtosis, and entropy measures. The unknown parameters of the proposed distribution are estimated using the well-known maximum-likelihood method. A simulation experiment is evaluated to assess the effectiveness of the applied estimation method. Finally, the superiority and flexibility of the newly presented distribution are examined by analyzing two real data sets. The application of the proposed model is compared with other existing probability distributions, and based on specific evaluation criteria, we observe that the proposed distribution offers optimal fitting compared to other rival distributions.

1. Introduction

In the lifetime and environmental analysis, probability distributions play an essential role in the description and statistical analysis of real phenomena in nature, including economics, biomedicine, engineering, insurance, and behavioral sciences. Over the last few decades, several techniques have been proposed in the literature to create new classes of probability distributions by modifying classical distributions. This includes a variety of techniques, such as the transformation method, power distributions, compound distributions, and combining multiple distributions. Among the notable examples are the exponentiated family introduced by Medholkar and Srivastava [1], the Marshal-Olkin generated family of probability distribution presented by Marshal and Olkin [2], the Beta-Generated family introduced by Eugene et al. [3], the transmuted extension defined by Shaw and Buckley [4], Gamma-generated family generated Zografos and Balakrishnan [5], the Kumaraswamy-Generated approach developed by Cordeiro and de Castro [6], Generalized beta-generated technique established Alexander et al. [7], the T-X method introduced by Alzaatreh et al. [8], the Weibull-G family defined by Bourguignon et al. [9], the compound exponential and gamma introduced by Meraou et al. [10, 11], the new version of Nadarajah-Haghighi model Almetwally and Meraou [12], a new aditive family of distributions provided by Mahdavi and Kundu [13], and several others.

However, recent studies suggest that classical distributions often require improvement. Due to this restriction, there is a need for more flexible versions of these distributions, which has resulted in notable progress in the generalization of well-established models. In applications spanning these domains, these extended distributions have proven successful. Among the available set of distributional generalizations is the new odd type-G family (NOT-G), which is introduced by Sapkota et al. [14]. The suggested family can introduce more probability distributions by including two additional parameters in the base distributions, and it is very versatile, offering a suitable fit to the considered real data sets. Its cumulative distribution function (cdf) $F\left(x;\lambda,\boldsymbol{\hbar}\right)$ is expressed as follows:

$$F\left(x;\boldsymbol{\hbar}\right) = (1+\delta)^{\eta}\left[\frac{H(x;\boldsymbol{\hbar})}{\delta + H(\boldsymbol{x};\boldsymbol{\hbar})}\right]^{\eta}, \qquad x \in \mathbb{R}, \delta, \eta > 0, \tag{1.1}$$

Considering the computation of $\frac{d}{dx}F\left(x;\boldsymbol{\hbar}\right)$, brings us to the mathematical form of the probability density function (pdf), denoted as $f\left(x;\boldsymbol{\hbar}\right)$, which is represented as follows:

$$f\left(x;\boldsymbol{\hbar}\right) = \delta\eta(1+\delta)^{\eta}\left[\frac{H(x;\boldsymbol{\hbar})^{\eta-1}}{(\delta + H(\boldsymbol{x};\boldsymbol{\hbar}))^{\eta+1}}\right] h(x;\boldsymbol{\hbar}). \tag{1.2}$$

In most scenarios, the inverse Rayleigh distribution (IRD), introduced by Smadi and Alrefaei [15], has demonstrated an optimal fit for real-world events, such as those in medicine, engineering, insurance, and risk management. The IRD has received considerable attention in the literature; for example, see the studies by Fatima and Ahmad [16], Shala and Merovci cite Sha, Mukherjee and Maiti [18], and Soliman et al. [19]. The mathematical description of the CDF of the IRD is as follows:

$$G\left(y;\theta\right) = e^{-\frac{\theta^2}{y^2}}, \qquad y > 0, \theta > 0. \tag{1.3}$$

Considering the computation of $\frac{d}{dy}G\left(y;\theta\right)$, the mathematical description of the pdf, say $g\left(y;\theta\right)$that it takes the form below:

$$g\left(y;\theta\right) = \frac{2\theta^2}{t^3}\, e^{-\frac{\theta^2}{y^2}}. \tag{1.4}$$

It is essential to demonstrate the inherent adaptability and desirable properties of the NOT-IRD. Due to its ability to describe complex data structures, the NOT-IRD can be widely used in various statistical applications, notably reliability analysis, risk assessment, survival studies, environmental modeling, and insurance. In this study, we will concentrate on the application of the NOT-IRD in ecological analysis. In addition, another aim of this work is to estimate the model parameters using the well-known maximum likelihood estimation procedure, and we also obtain approximate confidence intervals for these parameters.

The current study, presented in this paper, is organized into several subsections. Section 2 focuses on proposing the distributional properties, accompanied by visual illustrations of the NOT-IRD. Section 3 elaborates on various statistical properties of the proposed model. Section 4 explains the point estimator for the NOT-IRD using the MLE method, supported by simulation analyses. Section 5 demonstrates the applicability of the NOT-IRD to real-life data sets. Finally, Section 6 provides a summary of the paper.

2. Derivation of the new odd type-inverse Rayleigh distribution

Characterized by the parameters $\delta > 0$, $\eta > 0$, and $\theta > 0$, the cdf of the NOT-IRD can be obtained by inserting the cdf of the IRD (1.3) into Eq. (1.1)

$$\Omega(t;\boldsymbol{\Delta}) = (1+\delta)^{\eta}\left[\frac{e^{-\frac{\theta^2}{t^2}}}{\delta + e^{-\frac{\theta^2}{t^2}}}\right]^{\eta}, \quad t \geq 0. \tag{2.1}$$

The calculation of $\frac{d}{dt}\Omega(t;\boldsymbol{\Delta})$ results in the mathematical formulation of the pdf linked to the NOT-IRD. This pdf, represented as $\omega(t;\boldsymbol{\Delta})$, can be expressed as:

$$\omega(t;\boldsymbol{\Delta}) = \frac{2\theta^2\delta\eta}{t^3}(1+\delta)^{\eta}\left[\frac{e^{-\frac{\eta\theta^2}{t^2}}}{\left(\delta + e^{-\frac{\theta^2}{t^2}}\right)^{\eta+1}}\right]. \tag{2.2}$$

Figure (1) displays a collection of plots demonstrating the pdf of the NOT-IRD, for different values of $\boldsymbol{\Delta} = (\delta, \eta, \theta)$. The visual features shown in Figure (1) are leading to the right-skewed, unimodal, and decreasing features of $\omega(t;\boldsymbol{\Delta})$.

The development of the survival function (sf) for the NOT-IRD is computed with $1 - \Omega(t;\boldsymbol{\Delta})$, where $\Omega(t;\boldsymbol{\Delta})$ is presented in Eq. (2.1). This SF has the subsequent mathematical expression:

$$S(t;\boldsymbol{\Delta}) = 1 - (1+\delta)^{\eta}\left[\frac{e^{-\frac{\theta^2}{t^2}}}{\delta + e^{-\frac{\theta^2}{t^2}}}\right]^{\eta}. \tag{2.3}$$

Next, the cumulative hazard rate function (chrf) of the NOT-IRD is inserted by $-S(t;\boldsymbol{\Delta})$, with $S(t;\boldsymbol{\Delta})$ presented in Eq. (2.3). The chrf is expressed in the following mathematical format:

$$H(t;\boldsymbol{\Delta}) = -\log\left\{1 - (1+\delta)^{\eta}\left[\frac{e^{-\frac{\theta^2}{t^2}}}{\delta + e^{-\frac{\theta^2}{t^2}}}\right]^{\eta}\right\}.$$

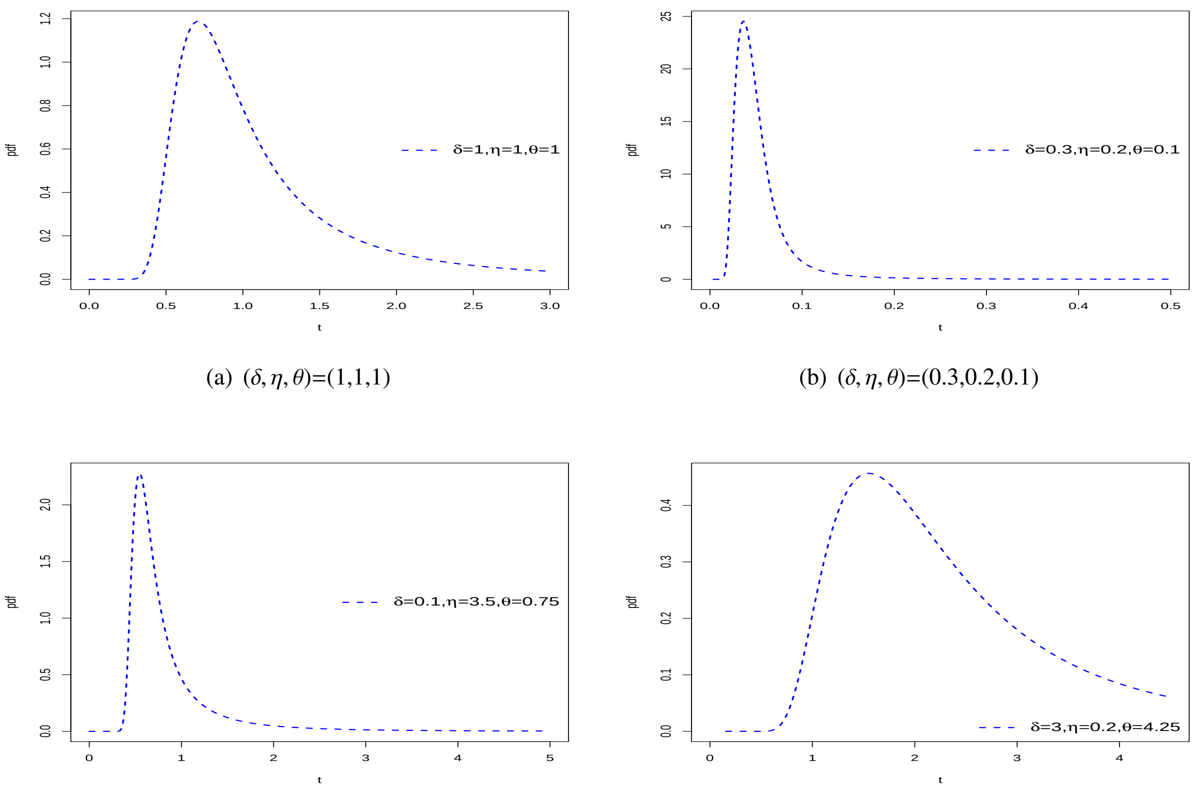

(a) (δ, η, θ)=(1,1,1)

(b) (δ, η, θ)=(0.3,0.2,0.1)

(c) (δ, η, θ)=(0.1,3.5,0.75)

(d) (δ, η, θ)=(3,0.2,4.25)

Figure 1. pdfs of the NOT-IRD for different values of $\boldsymbol{\Delta} = (\delta, \eta, \theta)$.

In addition, the evaluation of the ratio $\dfrac{\omega(t;\boldsymbol{\Delta})}{\Omega(t;\boldsymbol{\Delta})}$ leads to the mathematical formulation of the reverse hazard rate function (rhrf) linked to the NOT-IRD. The RHRF is expressed in the following mathematical manner:

$$r(t;\boldsymbol{\Delta}) = \frac{2\theta^2\delta\eta}{t^3\left(\delta + e^{-\frac{\theta^2}{t^2}}\right)}.$$

Finally, the mathematical expression of the hazard rate function (hrf) associated with the NOT-IRD is provided by the ratio of $\dfrac{\omega(t;\boldsymbol{\Delta})}{S(t;\boldsymbol{\Delta})}$. The hrf can be mathematically given as

$$h(t;\boldsymbol{\Delta}) = \frac{2\theta^2\delta\eta(1+\delta)^\eta\left[\dfrac{e^{-\frac{\eta\theta^2}{t^2}}}{\left(\delta + e^{-\frac{\theta^2}{t^2}}\right)^{\eta+1}}\right]}{t^3\left\{1-(1+\delta)^\eta\left[\dfrac{e^{-\frac{\theta^2}{t^2}}}{\delta + e^{-\frac{\theta^2}{t^2}}}\right]^\eta\right\}}. \tag{2.4}$$

Similarly, hrf of the NOT-IRD are graphically illustrated in Figure (2). The hrf of the NOT-IRD takes diverse shapes. It exhibits various non-monotonic shapes, including decreasing, reversed J shapes, and unimodal forms.

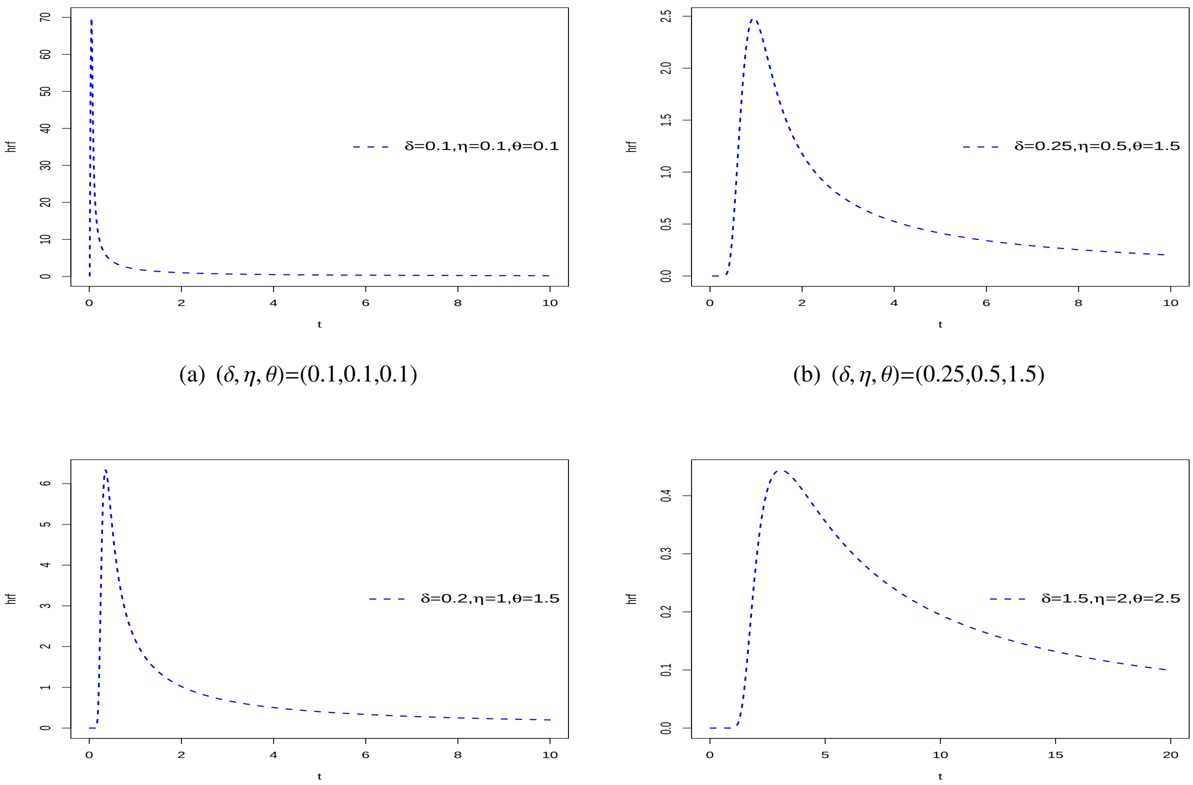

(a) (δ, η, θ)=(0.1,0.1,0.1) (b) (δ, η, θ)=(0.25,0.5,1.5)

(c) (δ, η, θ)=(0.2,1,1.5) (d) (δ, η, θ)=(1.5,2,2.5)

Figure 2. hrfs of the NOT-IRD for different values of $\boldsymbol{\Delta} = (\delta, \eta, \theta)$.

3. Some mathematical properties

This section derived several statistical properties of the recommended NOT-IRD. We introduced the mathematical formula of the quantile function (QF). We derived additional properties motivated by the quantile, such as skewness and kurtosis, moments and their related measures, entropy information, and order statistic distributions of the NOT-IRD.

3.1. Quntile function

The QF is a crucial tool used to investigate the probability distribution characteristics and generate random numbers. Another term for the QF is the inverse CDF. Let $T \in \mathbb{R}^{+}$ conforms to the NOT-IRD with cdf given in Eq. (2.1), its QF has following form:

$$t(q) = \left(-\theta^{2}\left\{\log\left[\frac{\delta q^{1/\eta}}{1+\delta-q^{1/\eta}}\right]\right\}^{-1}\right)^{\frac{1}{2}}, \qquad 0 < q < 1. \tag{3.1}$$

Furthermore, by using q as a uniform random number with interval $(0,1)$, the Eq. (3.1) can generate a random sample from any subcase of the NOT-IRD. Also, The median of the NOT-IRD is determined by setting $q=\frac{1}{4}$ in Eq. (3.1). Similarly, other quantiles can be calculated, including first and third quartiles by setting $q=\frac{1}{4}$ and $q=\frac{3}{4}$, respectively.

The importance of QF lies in its computation of skewness and kurtosis. As a result, we applied the Bowley Skewness γ_3 and the Moors' kurtosis γ_4, which are based on quartiles and are, respectively, defined by:

$$\gamma_3=\frac{t(3/4)+t(1/4)-2t(1/2)}{t(3/4)-t(1/4)},$$

and

$$\gamma_4=\frac{t(1/8)+t(3/8)+t(7/8)-t(5/8)}{t(3/4)-t(1/4)}.$$

3.2. *Useful expansion*

By the generalized binomial series for $b>0$ and $|x|<1$,

$$\left[\frac{x}{a+x}\right]^b=\sum_{l=0}^{\infty}(-1)^{l+1}\binom{b+l-1}{l}\left[\frac{a}{x}\right]^l,$$

We can write the CDF of the NOT-IRD as

$$\Omega(t;\mathbf{\Delta})=(1+\delta)^{\eta}\sum_{l=0}^{\infty}(-1)^{l+1}\binom{b+l-1}{l}\left(\frac{\delta}{e^{-\frac{\theta^2}{t^2}}}\right)^l$$

Consequently, the corresponding PDF of the NOT-IRD is

$$\omega(t;\mathbf{\Delta})=\frac{2\theta^2}{t^3}\,(1+\delta)^{\eta}\sum_{l=0}^{\infty}\Psi_l(\delta,\eta)\,\exp\left(\tfrac{l\,\theta^2}{t^2}\right),$$

with $\Psi_l(\delta,\eta)=(-1)^{l+1}\,l\,\delta^l\binom{\eta+l-1}{l}$.

3.3. r^{th} *moment*

By employing moments, we can calculate various statistical measures, such as the mean, variance, coefficient of variance, and index of dispersion, to summarize the shape and characteristics of a distribution. Moments are also useful for summarizing data, comparing probability distributions, and managing risks. Let T be a random variable that follows the NOT-IRD, then the r^{th} moment of T can be defined as

$$\begin{aligned}\mu_r^{'}&=\int_0^{\infty}t^r\,\omega(t;\mathbf{\Delta})\,dt=2\theta^2(1+\delta)^{\eta}\sum_{l=0}^{\infty}\Psi_l(\delta,\eta)\int_0^{\infty}t^{r-3}\,\exp\left(\tfrac{l\,\theta^2}{t^2}\right)\,dt\\&=2\theta^2(1+\delta)^{\eta}\sum_{l=0}^{\infty}\Psi_l(\delta,\eta)\,\Phi(t;r),\end{aligned}\tag{3.2}$$

where, $\Phi(t;r) = \int_0^{\infty} t^{r-3}\ \exp\left(\frac{l\,\theta^2}{t^2}\right)\ dt.$
Using equation (3.2), the mean $\mu_1^{'}$ and second moment $\mu_2^{'}$ of the NOT-IRD are as follows

$$\mu_1^{'} = 2\theta^2(1+\delta)^{\eta} \sum_{l=0}^{\infty} \Psi_l(\delta,\eta)\ \Phi(t;1),$$

and

$$\mu_2^{'} = 2\theta^2(1+\delta)^{\eta} \sum_{l=0}^{\infty} \Psi_l(\delta,\eta)\ \Phi(t;2).$$

The variance (σ^2) and index of dispersion (ID) of the NOT-IRD are given, respectively, as

$$\sigma^2 = \mu_2^{'} - (\mu_1^{'})^2,\ ID = \frac{\sigma^2}{\mu_1^{'}}.$$

Furthermore, the mathematical expression of the moment generating function (mgf) of the NOT-IRD, say $M_T(k)$, is derived as

$$M_T(k) = \int_0^{\infty} e^{kt}\ \omega(t;\mathbf{\Delta})\ dt = 2\theta^2(1+\delta)^{\eta} \sum_{l=0}^{\infty}\sum_{r=0}^{\infty} \frac{k^r}{r!}\Psi_l(\delta,\eta)\ \Phi(t;r).$$

The numerical description of the $\mu_1^{'}$, σ^2, ID, γ_3, and γ_4 of the special member of the introduced NOT-IRD with the combination of various parameter values is shown in Table (1). The same can easily be observed for these quantities from the plots presented in Figures (3) and (4). These results indicate that the NOT-IRD can accommodate modeling skewed and complex data.

3.4. *Entropy information of the NOT-IRD*

Entropy measures are a crucial concept in summarizing diverse data sets from various fields, including environmental science, insurance, biology, and survival mathematics. The most popular entropy information is Rényi entropy [20], Shannon's [21] entropy, and the Tsallis [22] entropy. In this section, we outline the measures for the NOT-IRD.
The Rényi entropy, say $\mathcal{I}_1$ of of a random variable T quantifies the variation of uncertainty associated with T. It takes the form

$$\begin{aligned}
\mathcal{I}_1 &= \frac{1}{1-\xi}\log\left(\int_0^{\infty} \omega^{\xi}(t;\mathbf{\Delta})\ dt\right) = \frac{1}{1-\xi}\log\left(\int_0^{\infty}\left[\frac{2\theta^2}{t^3}\ (1+\delta)^{\eta}\sum_{l=0}^{\infty}\Psi_l(\delta,\eta)\ \exp\left(\frac{l\,\theta^2}{t^2}\right)\right]^{\xi}\ dt\right) \\
&= \frac{1}{1-\xi}\log\left(\left[2\theta^2(1+\delta)^{\eta}\sum_{l=0}^{\infty}\Psi_l(\delta,\eta)\right]^{\xi}\int_0^{\infty} t^{-3\xi}\ \exp\left(\frac{l\,\theta^2\,\xi}{t^2}\right)\right)\ dt \\
&= \frac{1}{1-\xi}\log\left(\left[2\theta^2(1+\delta)^{\eta}\sum_{l=0}^{\infty}\Psi_l(\delta,\eta)\right]^{\xi}\ \Psi(t;\xi)\right),
\end{aligned}$$

with, $\Psi(t;\xi) = \int_0^{\infty} t^{-3\xi}\ \exp\left(\frac{l\,\theta^2\,\xi}{t^2}\right)\ dt.$

Table 1. Numerical description of the important measures of the NOT-IRD.

η		θ	$\mu_1^{'}$	σ^2	ID	γ_3	γ_4
1.4	δ=0.3	1.2	1.4058	3.4352	2.4436	0.304	3.9283
		1.4	1.6401	4.6757	2.8509	0.304	3.9283
		1.6	1.8744	6.107	3.2582	0.304	3.9283
		1.8	2.1087	7.7292	3.6654	0.304	3.9283
	δ=0.6	1.2	1.6793	5.6582	3.3694	0.31	3.5206
		1.4	1.9592	7.7015	3.931	0.31	3.5206
		1.6	2.2391	10.0591	4.4925	0.31	3.5206
		1.8	2.519	12.731	5.0541	0.31	3.5206
	δ=0.9	1.2	1.8388	7.1882	3.9092	0.311	3.3536
		1.4	2.1453	9.7839	4.5607	0.311	3.3536
		1.6	2.4517	12.779	5.2122	0.311	3.3536
		1.8	2.7582	16.1735	5.8637	0.311	3.3536
	δ=1.2	1.2	1.9453	8.3038	4.2686	0.3109	3.2615
		1.4	2.2696	11.3024	4.9800	0.3109	3.2615
		1.6	2.5938	14.7624	5.6915	0.3109	3.2615
		1.8	2.918	18.6836	6.4029	0.3109	3.2615
1.8	δ=0.3	1.2	1.5582	4.4329	2.8449	0.3123	3.8273
		1.4	11.8179	6.0337	3.3191	0.3123	3.8273
		1.6	2.0776	7.8807	3.7932	0.3123	3.8273
		1.8	2.3373	9.9741	4.2674	0.3123	3.8273
	δ=0.6	1.2	1.8773	7.293	3.8848	0.3146	3.4526
		1.4	2.1902	9.9266	4.5322	0.3146	3.4526
		1.6	2.5031	12.9653	5.1797	0.3146	3.4526
		1.8	2.816	16.4092	5.8271	0.3146	3.4526
	δ=0.9	1.2	2.0635	9.2594	4.4873	0.3139	3.3022
		1.4	2.4074	12.6031	5.2352	0.3139	3.3022
		1.6	2.7513	16.4612	5.9831	0.3139	3.3022
		1.8	3.0952	20.8337	6.731	0.3139	3.3022
	δ=1.2	1.2	2.1877	10.6926	4.8875	0.3131	3.2201
		1.4	2.5524	14.5539	5.7021	0.3131	3.2201
		1.6	2.917	19.0091	6.5167	0.3131	3.2201
		1.8	3.2816	24.0584	7.3313	0.3131	3.2201

Shannon's entropy, say $\mathcal{I}_2$ of the NOT-IRD has the form

$$\mathcal{I}_2 \;=\; \mathrm{E}\left(-\log\omega(t;\mathbf{\Delta})\right) = \mathrm{E}\left(-\log\left[\frac{2\theta^2}{t^3}\,(1+\delta)^\eta\sum_{l=0}^{\infty}\Psi_l(\delta,\eta)\,\exp\left(\tfrac{l\,\theta^2}{t^2}\right)\right]\right).$$

The Tsallis entropy, say $\mathcal{I}_3$ of the NOT-IRD is derived as

$$\begin{aligned}\mathcal{I}_3 \;&=\; \frac{1}{1-\xi}\left(1-\int_0^\infty \omega^\xi(t;\mathbf{\Delta})\,dt\right) = \frac{1}{1-\xi}\left(1-\int_0^\infty\left[\frac{2\theta^2}{t^3}\,(1+\delta)^\eta\sum_{l=0}^{\infty}\Psi_l(\delta,\eta)\,\exp\left(\tfrac{l\,\theta^2}{t^2}\right)\right]^\xi dw\right)\\ &=\; \frac{1}{1-\xi}\left\{1-\left[2\theta^2(1+\delta)^\eta\sum_{l=0}^{\infty}\Psi_l(\delta,\eta)\right]^\xi\,\Psi(t;\xi)\right\}.\end{aligned}$$

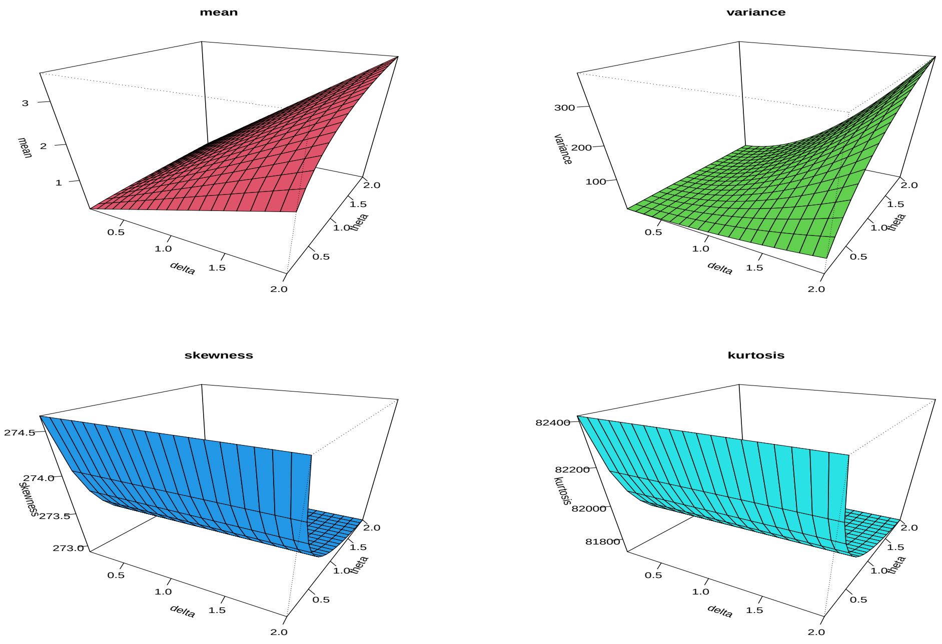

Figure 3. 3D graphical representations for several mathematical properties of NOT-IRD for various parameter values ($\eta = 1.4$).

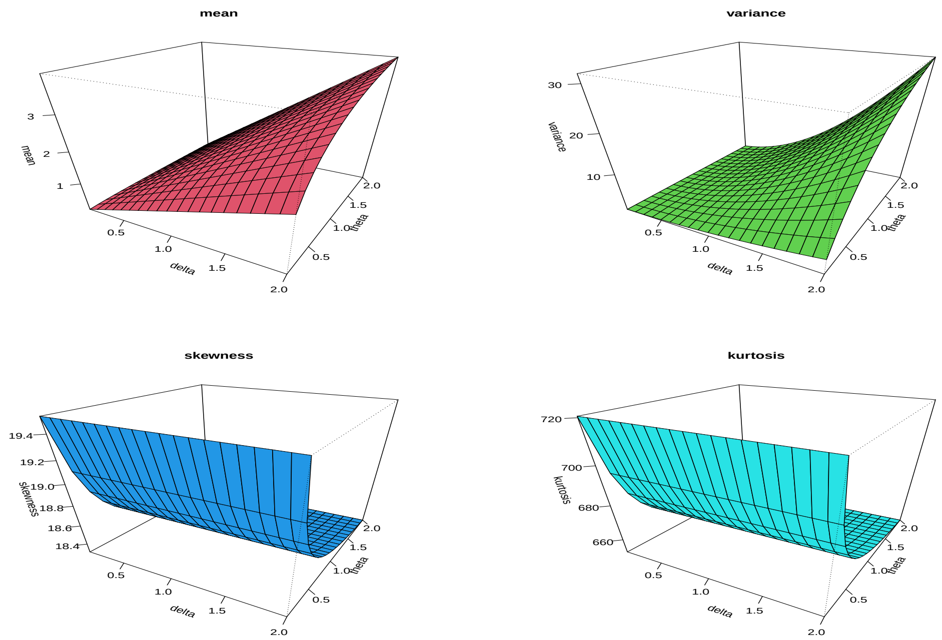

Figure 4. 3D graphical representations for several mathematical properties of NOT-IRD for various parameter values ($\eta = 1.8$).

Table (2) displays the numerical values of the $\mathcal{I}_1$, $\mathcal{I}_2$, and $\mathcal{I}_3$ of the NOT-IRD, calculated numerically for various parameter values using R software. From the Table (2), it is clear that all the proposed information entropy of the NOT-IRD can be either negative or positive. This indicates that the proposed NOT-IRD can make it a versatile option for modeling diverse sorts of data. In addition, Figures (5) and (6) support the same conclusion.

Table 2. Some descriptive entropy measures with diverse combinations of parameter values.

ξ	θ		δ	$\mathcal{I}_1$	$\mathcal{I}_2$	$\mathcal{I}_3$
0.9	0.45	η=0.4	0.5	-0.4916	-0.598	-0.4797
			1.0	-0.3127	-0.4327	-0.3079
			1.5	0.2302	-0.3573	-0.2276
		η=0.8	0.5	-0.2083	-0.3456	-0.2062
			1.0	-0.0029	-0.1582	-0.002
			1.5	0.0911	-0.0742	0.0915
		η=1.6	0.5	0.1053	-0.0693	0.1058
			1.0	0.3257	0.1216	0.3311
			1.5	0.4254	0.2047	0.4345
ξ = 1.8	θ = 2.5	η=0.4	0.5	0.8071	0.7050	0.5946
			1.0	0.968	0.7537	0.6738
			1.5	1.0428	0.7704	0.7073
		η=0.8	0.5	1.0473	0.7080	0.7092
			1.0	1.2476	0.7290	0.7893
			1.5	1.3403	0.7315	0.8222
		η=1.6	0.5	1.3407	0.9325	0.8223
			1.0	1.5643	0.9299	0.8924
			1.5	1.6661	0.9171	0.9204

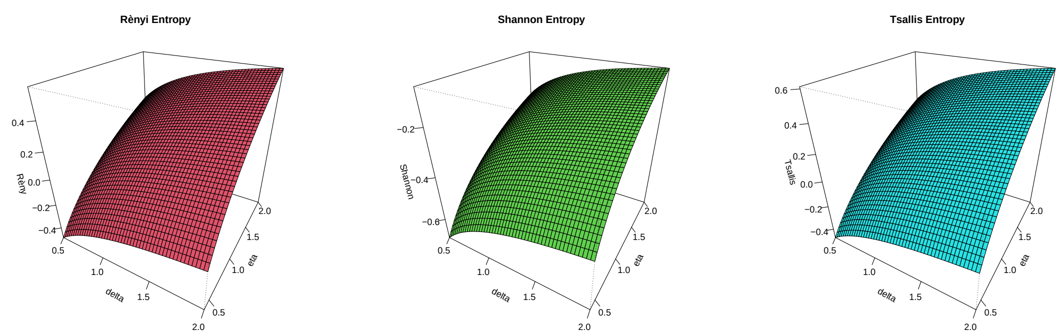

Figure 5. Plots of proposed entropy information of the NOT-IRD for for ξ = 0.9 and θ = 0.45.

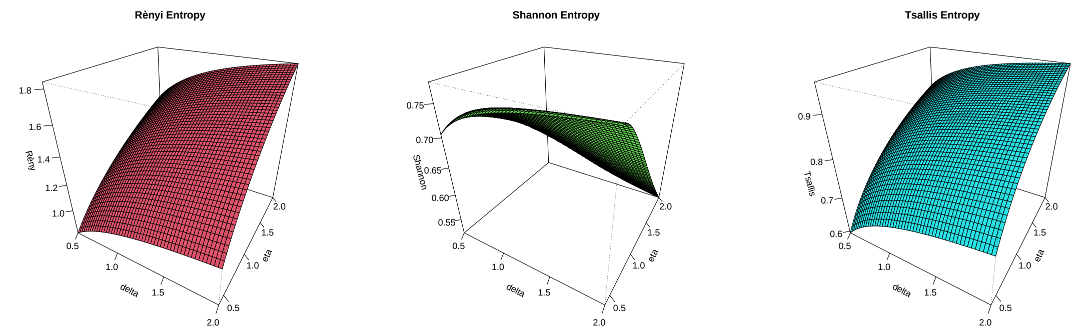

Figure 6. Plots of proposed entropy information of the NOT-IRD for $\xi = 1.8$ and $\theta = 2.5$.

3.5. Order statistics of the NOT-IRD

Let $T_1, T_2, ..., T_l$ be a random sample from Eq. (2.2), with the OS $T_{(1)}, T_{(2)}, ..., T_{(l)}$. It is well-established that the pdf of the j^{th} OS, denoted as $T_{(j)}$, is given (for $j = 1, 2, ..., l$) by

$$\begin{aligned}
\mu_{(j)}(t;\mathbf{\Delta}) &= \frac{l!\ \omega(t;\mathbf{\Delta})}{(j-1)!(l-j)!}\ [\Omega(t;\mathbf{\Delta})]^{j-1}\ [1-\Omega(t;\mathbf{\Delta})]^{l-j} \\
&= \frac{2\theta^2\ \delta\ \eta\ l!}{t^3(j-1)!(l-j)!}\ (1+\delta)^{j\ \eta} \left[\frac{e^{-\frac{\eta\theta^2}{t^2}}}{\left(\delta+e^{-\frac{\theta^2}{t^2}}\right)^{\eta+1}}\right]^j \left\{1-(1+\delta)^{\eta}\left[\frac{e^{-\frac{\theta^2}{t^2}}}{\delta+e^{-\frac{\theta^2}{t^2}}}\right]^{\eta}\right\}^{l-j}
\end{aligned}$$

The pdf of the 1^{st} and l^{th} OS of the NOT-IRD can be, respectively, stated as $T_{(1)} = \min\{T_1, T_2, ..., T_l\}$ and $T_{(*)} = \max\{T_1, T_2, ..., T_l\}$, and they can expressed as below

$$\mu_{(1)}(t;\mathbf{\Delta}) = \frac{2l\ \theta^2\ \delta\ \eta}{t^3}\ (1+\delta)^{j\ \eta} \left[\frac{e^{-\frac{\eta\theta^2}{t^2}}}{\left(\delta+e^{-\frac{\theta^2}{t^2}}\right)^{\eta+1}}\right]^j \left\{1-(1+\delta)^{\eta}\left[\frac{e^{-\frac{\theta^2}{t^2}}}{\delta+e^{-\frac{\theta^2}{t^2}}}\right]^{\eta}\right\}^{1-j},$$

and

$$\mu_{(l)}(t;\mathbf{\Delta}) = \frac{2l\ \theta^2\ \delta\ \eta}{t^3}\ (1+\delta)^{j\ \eta} \left[\frac{e^{-\frac{\eta\theta^2}{t^2}}}{\left(\delta+e^{-\frac{\theta^2}{t^2}}\right)^{\eta+1}}\right]^j.$$

4. Estimation and simulation

The whole contribution of this section is organized into two distinct subsections. The first subsection is reserved for the mathematical derivation of the MLEs of the NOT-IRD, with the construction of the confidence interval for the model parameters. In the second subsection, we shift our focus to the analytical evaluation of the estimated parameters using simulation studies that explore various configurations for the vector parameter $\mathbf{\Delta} = (\delta, \eta, \theta)$.

4.1. Maximum likelihood estimation

Let $T_1, T_2, \ldots, T_l$ represent a random collection of samples drawn from $\omega(t_i; \mathbf{\Delta})$ as outlined in Eq. (2.2), with the corresponding observed values denoted by $t_1, t_2, \ldots, t_l$. In this context, we can construct the likelihood function (LF), denoted as $\mathcal{L}\left(\underline{t}; \mathbf{\Theta}\right)$, by utilizing the observed samples $T_1, T_2, \ldots, T_l$ in conjunction with the specified $\omega(t_i; \mathbf{\Delta})$. Thus, the LF $\mathcal{L}\left(\underline{t}; \mathbf{\Theta}\right)$, is formulated as follows:

$$\mathcal{L}\left(\underline{t}; \mathbf{\Delta}\right) = \prod_{i=1}^{l} \omega(t_i; \mathbf{\Delta}). \tag{4.1}$$

By incorporating $\omega(t_i; \mathbf{\Delta})$ from Eq. (2.2) in Eq. (4.1) results in the following outcome:

$$\mathcal{L}\left(\underline{t}; \mathbf{\Delta}\right) = \prod_{i=1}^{l} \frac{2\theta^2 \delta\eta}{t_i^3} (1+\delta)^{\eta} \left[\frac{e^{-\frac{\eta\theta^2}{t_i^2}}}{\left(\delta + e^{-\frac{\theta^2}{t_i^2}}\right)^{\eta+1}} \right]. \tag{4.2}$$

In relation to $\mathcal{L}\left(\underline{t}; \mathbf{\Theta}\right)$ as presented in Eq. (4.2), the logarithmic LF, after omitting the constant terms, is denoted as $\mathcal{L}\left(\underline{t}; \mathbf{\Theta}\right)$, and can be expressed as follows:

$$\mathcal{LL}\left(\underline{t}; \mathbf{\Delta}\right) = l \log(2\theta^2 \delta\eta) - \sum_{i=1}^{l} t_i^{-3} + l\eta \log(1+\delta) - \eta\theta^2 \sum_{i=1}^{l} t_i^{-2} - (\eta+1) \sum_{i=1}^{l} \log\left(\delta + e^{-\frac{\theta^2}{t_i^2}}\right). \tag{4.3}$$

To obtain the MLEs of parameters, we differentiate (4.3) partially with respect to δ, η, and θ and equating them to zero, we get the following three equations:

$$\frac{\partial}{\partial\delta} \mathcal{LL}\left(\underline{t}; \mathbf{\Delta}\right) = \frac{l}{\delta} - \frac{l\eta}{1+\delta} - (\eta+1) \sum_{i=1}^{l} \left(\delta + e^{-\frac{\theta^2}{t_i^2}}\right)^{-1}$$

$$\frac{\partial}{\partial\eta} \mathcal{LL}\left(\underline{t}; \mathbf{\Delta}\right) = \frac{l}{\eta} + l \log(1+\delta) - \theta^2 \sum_{i=1}^{l} t_i^{-2} - \sum_{i=1}^{l} \log\left(\delta + e^{-\frac{\theta^2}{t_i^2}}\right)$$

and

$$\frac{\partial}{\partial\theta} \mathcal{LL}\left(\underline{t}; \mathbf{\Delta}\right) = \frac{2l}{\theta} - 2\eta\theta \sum_{i=1}^{l} t_i^{-2} + 2\theta(\eta+1) \sum_{i=1}^{l} \frac{e^{-\frac{\theta^2}{t_i^2}}}{t_i^2 \left(\delta + e^{-\frac{\theta^2}{t_i^2}}\right)}.$$

Then the MLEs of the parameters $\mathbf{\Delta} = (\delta, \eta, \theta)$, denoted by $\hat{\mathbf{\Delta}} = (\hat{\delta}, \hat{\eta}, \hat{\theta})$ respectively are obtained by solving the above three equations simultaneously. These equations cannot be solved analytically, and statistical software can be used to solve them numerically via iterative methods, such as the Newton-Raphson, bisection, or fixed-point techniques.

Additionally, another aspect of inference involves producing the confidence interval (CI) for the unknown parameters. For this, Let $\mathbf{\Delta} = (\delta, \eta, \eta)$ be the vector parameter. The asymptotic distribution of MLEs is structured by

$$\left(\hat{\mathbf{\Delta}} - \mathbf{\Delta}\right) \sim \mathbf{N}(0, \mathbf{S}^{-1}(\mathbf{\Delta})),$$

with $\mathbf{S^{-1}}(\boldsymbol{\Delta})$ is the variance-covariance matrix for $\boldsymbol{\Delta}$. The elements of 3×3 matrix $\mathbf{S}^{-1}$, which is

$$\mathbf{S}(\Xi) = -\begin{pmatrix} \frac{\partial^2}{\partial\delta^2}\mathcal{LL}\left(\underline{t};\boldsymbol{\Delta}\right) & \frac{\partial}{\partial\delta\partial\eta}\mathcal{LL}\left(\underline{t};\boldsymbol{\Delta}\right) & \frac{\partial}{\partial\delta\partial\theta}\mathcal{LL}\left(\underline{t};\boldsymbol{\Delta}\right) \\ \frac{\partial}{\partial\eta\partial\delta}\mathcal{LL}\left(\underline{t};\boldsymbol{\Delta}\right) & \frac{\partial^2}{\partial\eta^2}\mathcal{LL}\left(\underline{t};\boldsymbol{\Delta}\right) & \frac{\partial}{\partial\eta\partial\theta}\mathcal{LL}\left(\underline{t};\boldsymbol{\Delta}\right) \\ \frac{\partial}{\partial\theta\partial\delta}\mathcal{LL}\left(\underline{t};\boldsymbol{\Delta}\right) & \frac{\partial}{\partial\theta\partial\eta}\mathcal{LL}\left(\underline{t};\boldsymbol{\Delta}\right) & \frac{\partial^2}{\partial\theta^2}\mathcal{LL}\left(\underline{t};\boldsymbol{\Delta}\right) \end{pmatrix}$$

As a result, the $100(1-\alpha)\%$ approximate CI for $\boldsymbol{\Delta}$ is obtained to be

$$\left[\hat{\boldsymbol{\Delta}}_j \pm N_{1-\alpha/2}\sqrt{\mathbf{S^{-1}_{jj}}}\right], \quad j = 1,2,3,$$

with $N_{1-\alpha/2}$ is the standard normal distribution N(0,1).

4.2. Least Square estimation

Let $t_{(1:l)},\ldots,t_{(l:l)}$ be considered an ordered sample from NOT-IRD. The LS estimates of $\boldsymbol{\Delta} = (\delta,\eta,\theta)$, denoted by $\hat{\boldsymbol{\Delta}}_{LSE} = (\hat{\delta}_{LSE},\hat{\eta}_{LSE},\hat{\theta}_{LSE})$ can be computed, respectively, as minimize the below function

$$\begin{aligned} \mathcal{LSE}(\boldsymbol{\Delta}|\mathrm{t}) &= \sum_{k=1}^{l}\left[\Omega(t_{(k:l)}|\boldsymbol{\Delta}) - \frac{k}{l+1}\right]^2 \\ &= \sum_{k=1}^{l}\left[(1+\delta)^{\eta}\left[\frac{e^{-\frac{\theta^2}{t^2_{(k:l)}}}}{\delta + e^{-\frac{\theta^2}{t^2_{(k:l)}}}}\right]^{\eta} - \frac{k}{l+1}\right]^2, \end{aligned}$$

The solution of the resulting nonlinear equations determine the final estimates of $\hat{\boldsymbol{\Delta}}_{LSE}$, which are

$$\sum_{k=1}^{l}\left[(1+\delta)^{\eta}\left[\frac{e^{-\frac{\theta^2}{t^2_{(k:l)}}}}{\delta + e^{-\frac{\theta^2}{t^2_{(k:l)}}}}\right]^{\eta} - \frac{k}{l+1}\right]\phi_1(t_{(k:l)}|\boldsymbol{\Delta}) = 0,$$

$$\sum_{k=1}^{l}\left[(1+\delta)^{\eta}\left[\frac{e^{-\frac{\theta^2}{t^2_{(k:l)}}}}{\delta + e^{-\frac{\theta^2}{t^2_{(k:l)}}}}\right]^{\eta} - \frac{k}{l+1}\right]\phi_2(t_{(k:l)}|\boldsymbol{\Delta}) = 0,$$

and

$$\sum_{k=1}^{l}\left[(1+\delta)^{\eta}\left[\frac{e^{-\frac{\theta^2}{t^2_{(k:l)}}}}{\delta + e^{-\frac{\theta^2}{t^2_{(k:l)}}}}\right]^{\eta} - \frac{k}{l+1}\right]\phi_3(t_{(k:l)}|\boldsymbol{\Delta}) = 0,$$

where

$$\phi_1(t_{(k:l)}|\boldsymbol{\Delta}) = \frac{\partial}{\partial\delta}\Omega(t_{(k:l)}|\boldsymbol{\Delta}), \tag{4.4}$$

$$\phi_2(t_{(k:l)}|\boldsymbol{\Delta}) = \frac{\partial}{\partial\eta}\Omega(t_{(k:l)}|\boldsymbol{\Delta}), \tag{4.5}$$

and

$$\phi_3(t_{(k:l)}|\boldsymbol{\Delta}) = \frac{\partial}{\partial\theta}\Omega(t_{(k:l)}|\boldsymbol{\Delta}). \tag{4.6}$$

4.3. Maximum product of spacings estimation

Let $t_{(1:l)}, \ldots, t_{(l:l)}$ represent the ordered statistics derived from our proposed NOT-IRD. The spacing distance is defined as follows

$$M_k(\boldsymbol{\Delta}) = \Omega(t_{(k:l)}|\boldsymbol{\Delta}) - \Omega(t_{(k-1:l)}|\boldsymbol{\Delta}), k = 1, \ldots, l+1,$$

with, $\Omega(t_{(0:l)}|\boldsymbol{\Delta}) = 0$ and $\Omega(t_{(l+1:l)}|\boldsymbol{\Delta}) = 1$. As a result $\sum_{k=1}^{l+1} M_k(\boldsymbol{\Delta}) = 1$.

Henceforth, the MPS estimates $\hat{\boldsymbol{\Delta}}_{MPS}$ of $\boldsymbol{\Delta}$ can be computed according to solve the three nonlinear equations

$$\frac{\partial}{\partial \delta} M_k(\boldsymbol{\Delta}) = \frac{1}{l+1} \sum_{k=1}^{l+1} \frac{1}{M_k}(\boldsymbol{\Delta}) \left[\phi_1(t_{(k:l)}|\boldsymbol{\Delta}) - \phi_1(t_{(k-1:l)}|\boldsymbol{\Delta})\right] = 0,$$

$$\frac{\partial}{\partial \eta} M_k(\boldsymbol{\Delta}) = \frac{1}{l+1} \sum_{k=1}^{l+1} \frac{1}{M_k}(\boldsymbol{\Delta}) \left[\phi_2(t_{(k:l)}|\boldsymbol{\Delta}) - \phi_2(t_{(k-1:l)}|\boldsymbol{\Delta})\right] = 0,$$

and

$$\frac{\partial}{\partial \theta} M_k(\boldsymbol{\Delta}) = \frac{1}{l+1} \sum_{k=1}^{l+1} \frac{1}{M_k}(\boldsymbol{\Delta}) \left[\phi_3(t_{(k:l)}|\boldsymbol{\Delta}) - \phi_3(t_{(k-1:l)}|\boldsymbol{\Delta})\right] = 0.$$

4.4. Simulation analysis

This subsection will focus on the second objective, which is to present a Monte Carlo (MC) simulation analysis to evaluate the practical behavior of the MLE, LSE, and MPS methods for the NOT-IRD. We produce random numbers of different sizes, namely $l = 30, 50, 100, 200$, using the QF expression specified in Eq. (3.1), and three different sets of the combination of different parameter values, such as set I $= \boldsymbol{\Delta} = (0.25, 0.5, 0.75)$, set II $= \boldsymbol{\Delta} = (0.5, 0.75, 1)$, and set III $= \boldsymbol{\Delta} = (0.75, 1, 1.5)$ are analyzed to investigate the simulation result. In this study, each simulation procedure is repeated $N = 1000$ times, and we adopt three established metrics as evaluation criteria to assess the performance of the MLEs $\hat{\boldsymbol{\Delta}} = (\hat{\delta}, \hat{\eta}, \hat{\theta})$. The following formulas mathematically describe these metrics:

- Average estimate (AE)

$$AE\left(\boldsymbol{\Delta}\right) = \frac{1}{N} \sum_{i=1}^{N} \hat{\boldsymbol{\Delta}}_i$$

- Mean square error (MSE)

$$MSE\left(\boldsymbol{\Delta}\right) = \frac{1}{N} \sum_{i=1}^{N} \left(\boldsymbol{\Delta}_i - \boldsymbol{\Delta}\right)^2.$$

  and

- Bias

$$Bias\left(\boldsymbol{\Delta}\right) = \frac{1}{N} \sum_{i=1}^{N} \mid \boldsymbol{\Delta}_i - \boldsymbol{\Delta} \mid,$$

Tables (3)-(5) present numerical results from the analysis of simulation studies. In addition, the simulation descriptions (for the MSEs values) for sets I, II, and III are graphically presented, respectively, in Figures (7), (8), and (9).

In the end, the CIs of the model parameters of the NOT-IRD are constructed using the approximate method with a 95% confidence level. We adopt four established metrics as evaluation criteria, including the lower confidence level (LCL), upper confidence level (UCL), average length (AL), and coverage probabilities (CP). The results are summarized in numerical form in Table 6. From the MC simulation analysis, we have observed the following output:

1. As the sample size l increases, the MLE estimates grow the true value for all parameters. This confirms that the estimators obtained by the MLE technique are consistent and asymptotically unbiased.
2. As the sample size l increases, for all parameters, the value of MSEs and bias decreases and approaches zero. This ensures that the estimators obtained by the MLE technique are convergent.
3. With an increasing value of $\boldsymbol{\Delta}$, the MSE values increase.
4. Another aspect observed from the results obtained is that the CIs established based on the approximate method are very close in terms of the AL criterion for all parameters δ, η and θ.
5. All estimators obtained by the MLE technique have the highest CPs.

5. Application to environmental data sets

In this section, the supremacy and versatility of the newly proposed NOT-IRD are illustrated by analyzing two different real datasets from the environmental sector. A detailed explanation of these considered data sets is presented in the following subsection.

5.1. Data set I

The first real data set (i.e., environmental data) consists of 128 observations. It signifies the influence of soil fertility on the characterization of the biological fixation of $N2$ for Dimorphandra wilsonii frizz growth. The suggested dataset studied by Oliveira et al. [23]. For 128 plants, the values of the phosphorus concentration are recorded in Table (7).

5.2. Data set II

The second real data set (i.e., precipitation data) consists of 45 observations and signifies the maximum annual flood discharges of the North Saskatchewan over a period of 45 years. The proposed data set studied by Van Montfort [24], and its values are summarized in Table (8).
Corresponding to the respective data sets, some visual illustrations including kernel density, TTT (total test time), probability-probability (PP) plot, QQ plot, histogram, and box plot are envisaged in Figures (10) and (11) respectively. Further, Table (9) reported somme summary statistics values for the two recommended data sets.
To compare their suitability and flexibility with the newly introduced NOT-IRD, various competing models are assessed, such as Poisson generalized Rayleigh (PGRD), exponentiated generalized moment exponential (EGME), Poisson Lindley (PLD), inverse Rayleigh (IRD), exponential (Exp), and Rayleigh (RD), new odd type exponential (NOT-ED), and new odd type Rayleigh (NOT-RD) models.
The practical performances of the NOT-IRD and other contender distributions are analyzed by considering specific analytical measures. These measures comprised Akaike Information Criterion ($\mathcal{AIC}$), Bayesian Information Criterion ($\mathcal{BIC}$), Kolmogorov-Smirnov ($\mathcal{KS}$) statistics with its associated $\mathcal{P}$-values. These metrics are frequently used to evaluate the accuracy of the fit. These measures are calculated as follows:

$$\mathcal{AIC} = -2\log(\mathcal{LL}) + 2q,$$

$$\mathcal{BIC} = -2\log(\mathcal{LL}) + l\log(l).$$

and

$$\mathcal{KS} = \sup\left[\max_{1\le i\le l} \mid \frac{i}{l} - F_0(t_{(i)}) \mid, \max_{1\le i\le l} \mid F_0(t_{(i)}) - \frac{i-1}{l} \mid\right],$$

In the above mathematical expressions, l denotes the sample size, $\mathcal{LL}$ signifies the log-likelihood function, and q signifies the number of corresponding model parameters.

Table 3. The analytical examination of the unknown parameters of the NOT-IRD for set I.

Method	l	Par	AEs	MSEs	Biases
MLE	30	δ	0.1976	0.1147	0.0523
		η	0.6426	0.2087	0.1426
		θ	0.8533	0.4186	0.1033
	50	δ	0.1970	0.0493	0.0529
		η	0.5936	0.1141	0.0936
		θ	0.8160	0.2424	0.0660
	100	δ	0.2192	0.0152	0.0307
		η	0.5310	0.0356	0.0310
		θ	0.7654	0.1129	0.0154
	200	δ	0.2380	0.0097	0.0119
		η	0.5460	0.0375	0.0460
		θ	0.7493	0.0208	0.0006
MPS	30	δ	0.3436	0.0936	0.0887
		η	0.5149	0.0349	0.0862
		θ	0.8138	0.0638	0.0516
	50	δ	0.3064	0.0364	0.0410
		η	0.4955	0.0245	0.0628
		θ	0.7979	0.0479	0.0363
	100	δ	0.3013	0.0113	0.0222
		η	0.5147	0.0147	0.0394
		θ	0.7651	0.0151	0.015
	200	δ	0.2485	0.0015	0.0054
		η	0.4810	0.0109	0.0244
		θ	0.7835	0.0135	0.0093
LSE	30	δ	0.3252	0.0752	0.0677
		η	0.4792	0.0208	0.0117
		θ	0.7778	0.0278	0.0096
	50	δ	0.3146	0.0646	0.0536
		η	0.5106	0.0106	0.0282
		θ	0.7608	0.0108	0.0107
	100	δ	0.3193	0.0493	0.0360
		η	0.4955	0.0045	0.0062
		θ	0.7535	0.0035	0.0032
	200	δ	0.2411	0.0089	0.0074
		η	0.5077	0.0037	0.0181
		θ	0.7706	0.0026	0.008

Among the fitted distributions, a distribution that has the lowest values of these $\mathcal{AIC}$ and $\mathcal{BIC}$, and the highest $\mathcal{P}$ p-value will be the best-suited model with a superior fit for the considered data sets.

Table 4. The analytical examination of the unknown parameters of the NOT-IRD for set II.

Method	l	Par	AEs	MSEs	Biases
		δ	0.5850	0.3613	0.0850
	30	η	0.8300	0.3180	0.0800
		θ	1.1553	0.2439	0.1553
		δ	0.4230	0.0813	0.0769
MLE	50	η	0.8519	0.2752	0.1019
		θ	1.0817	0.1694	0.0817
		δ	0.4774	0.0647	0.0225
	100	η	0.7777	0.1300	0.0277
		θ	1.0610	0.0887	0.0610
		δ	0.5270	0.0308	0.0270
	200	η	0.7399	0.0495	0.0100
		θ	1.0218	0.0528	0.0218
		δ	0.6952	0.1952	0.2736
	30	η	0.7962	0.0462	0.1996
		θ	1.0687	0.1687	0.0991
		δ	0.6884	0.1884	0.2993
MPS	50	η	0.7352	0.0148	0.1909
		θ	1.1157	0.1157	0.1063
		δ	0.5196	0.0196	0.0769
	100	η	0.7325	0.0115	0.1344
		θ	1.0901	0.0901	0.064
		δ	0.5542	0.0142	0.044
	200	η	0.7513	0.0013	0.0705
		θ	1.0382	0.0382	0.0294
		δ	0.6678	0.1678	0.2266
	30	η	0.7632	0.0432	0.0331
		θ	1.0115	0.1115	0.0244
		δ	0.6235	0.1235	0.163
LSE	50	η	0.7938	0.0138	0.0192
		θ	0.9868	0.0932	0.0143
		δ	0.5817	0.0817	0.1408
	100	η	0.7471	0.0029	0.0561
		θ	1.0368	0.0368	0.0302
		δ	0.5725	0.0725	0.0597
	200	η	0.7399	0.0019	0.0125
		θ	1.0064	0.0064	0.0069

The estimated values, $\mathcal{AIC}$, $\mathcal{BIC}$, $\mathcal{KS}$, and $\mathcal{P}$-value of the NOT-IRD and other contender models are recorded in Tables (10). From these results, it is observed that the NOT-IRD has the lowest proposed metrics $\mathcal{AIC}$, $\mathcal{BIC}$, $\mathcal{KS}$, and the highest $\mathcal{P}$-value,

Table 5. The analytical examination of the unknown parameters of the NOT-IRD for set III.

Method	l	Par	AEs	MSEs	Biases
MLE	30	δ	0.7165	0.5111	0.0334
		η	1.3092	0.5703	0.3092
		θ	1.6367	0.2662	0.1367
	50	δ	0.7897	0.4833	0.0397
		η	1.2444	0.5068	0.2444
		θ	1.6338	0.2281	0.1338
	100	δ	0.7289	0.1697	0.0210
		η	1.0683	0.1936	0.0683
		θ	1.5693	0.0700	0.0693
	200	δ	0.7553	0.1055	0.0053
		η	1.0264	0.1235	0.0264
		θ	1.4731	0.0562	0.0268
MPS	30	δ	0.9856	0.2356	0.4502
		η	0.9572	0.0828	0.2227
		θ	1.6804	0.1804	0.2141
	50	δ	1.0528	0.2028	0.4196
		η	0.9359	0.0641	0.1787
		θ	1.6033	0.1033	0.1525
	100	δ	0.8443	0.0943	0.1557
		η	0.9220	0.0580	0.132
		θ	1.6257	0.0957	0.108
	200	δ	0.8708	0.0708	0.1207
		η	0.9185	0.0415	0.066
		θ	1.5751	0.0451	0.0545
LSE	30	δ	0.8693	0.1193	0.3425
		η	1.0972	0.0972	0.0541
		θ	1.5040	0.1404	0.0534
	50	δ	0.9076	0.1076	0.3639
		η	1.0641	0.0641	0.0786
		θ	1.5199	0.1199	0.0705
	100	δ	0.9143	0.0943	0.2947
		η	1.0688	0.0588	0.0385
		θ	1.4770	0.0530	0.0307
	200	δ	0.7658	0.0158	0.0741
		η	1.0133	0.0133	0.0288
		θ	1.5260	0.0260	0.0266

which ensures that the NOT-IRD is the optimal choice for modeling the two environmental data sets. Furthermore, Figures (12)-(15) present the fitted functions for the NOT-IRD with the fitting models, including the pdf, cdf, and sf using the two

Table 6. The CIs with associated CPs of the unknown parameters of the NOT-IRD for set I, II, and III.

Set	l	Par	LCLs	UCLs	ALs	CPs
I	30	δ	0.1135	0.4266	0.3130	0.91
		η	0.2205	0.9164	0.6959	0.94
		θ	0.5278	21.1015	0.5736	0.93
	50	δ	0.0090	0.7717	0.7626	0.95
		η	0.1400	1.2286	1.0886	0.97
		θ	0.3489	2.0329	1.6840	0.96
	100	δ	0.0370	0.5314	0.4943	0.97
		η	0.2243	0.9362	0.7119	0.98
		θ	0.3595	1.3416	0.9821	0.97
	200	δ	0.1135	0.4266	0.3130	0.97
		η	0.2205	0.9164	0.6959	0.99
		θ	0.5278	1.1015	0.5736	0.98
II	30	δ	0.0566	1.9504	1.8937	0.92
		η	0.1241	1.8692	1.745	0.93
		θ	0.6767	2.2588	1.5821	0.92
	50	δ	0.0894	1.0760	0.9866	0.94
		η	0.1742	2.1723	1.9980	0.96
		θ	0.7243	1.9008	1.1765	0.95
	100	δ	0.1682	1.0989	0.9306	0.96
		η	0.2411	1.4730	1.2318	0.98
		θ	0.7786	1.6247	0.8461	0.96
	200	δ	0.2651	0.9034	0.6382	0.98
		η	0.3866	1.0519	0.6652	0.99
		θ	0.8641	1.2991	0.4349	0.97
III	30	δ	0.0566	1.9504	1.8937	0.92
		η	0.1241	1.8692	1.745	0.93
		θ	0.6767	2.2588	1.5821	0.92
	50	δ	0.0894	1.0760	0.9866	0.94
		η	0.1742	2.1723	1.9980	0.96
		θ	0.7243	1.9008	1.1765	0.95
	100	δ	0.1682	1.0989	0.9306	0.96
		η	0.2411	1.4730	1.2318	0.98
		θ	0.7786	1.6247	0.8461	0.96
	200	δ	0.2651	0.9034	0.6382	0.98
		η	0.3866	1.0519	0.6652	0.99
		θ	0.8641	1.2991	0.4349	0.97

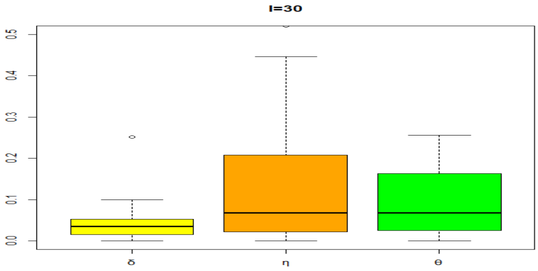

(a) l=30

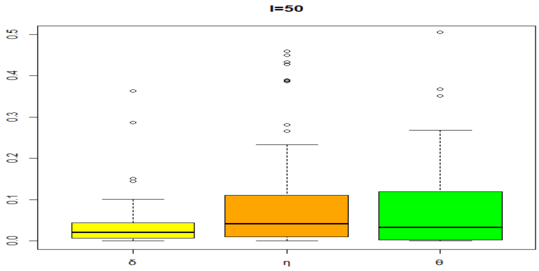

(b) l=50

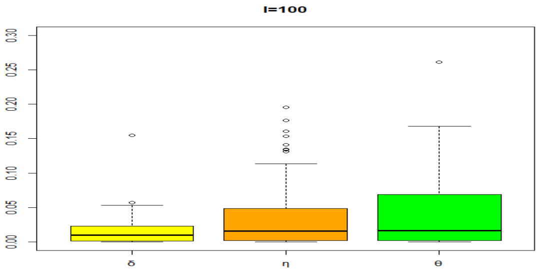

(c) l=100

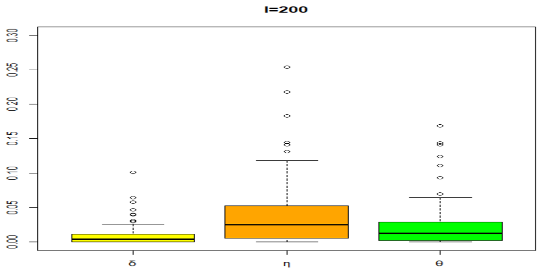

(d) l=200

Figure 7. Box plots for the MSEs of of $\mathbf{\Delta} = (\delta, \eta, \theta)$ using set I.

Table 7. Phosphorus concentration data.

0.22	0.17	0.11	0.10	0.15	0.06	0.05	0.07	0.12	0.09	0.23	0.25	0.23
0.24	0.20	0.08	0.11	0.12	0.10	0.06	0.20	0.17	0.20	0.11	0.16	0.09
0.10	0.12	0.12	0.10	0.09	0.17	0.19	0.21	0.18	0.26	0.19	0.17	0.18
0.20	0.24	0.19	0.21	0.22	0.17	0.08	0.08	0.06	0.09	0.22	0.23	0.22
0.19	0.27	0.16	0.28	0.11	0.10	0.20	0.12	0.15	0.08	0.12	0.09	0.14
0.07	0.09	0.05	0.06	0.11	0.16	0.20	0.25	0.16	0.13	0.11	0.11	0.11
0.08	0.22	0.11	0.13	0.12	0.15	0.12	0.11	0.11	0.15	0.10	0.15	0.17
0.14	0.12	0.18	0.14	0.18	0.13	0.12	0.14	0.09	0.10	0.13	0.09	0.11
0.11	0.14	0.07	0.07	0.19	0.17	0.18	0.16	0.19	0.15	0.07	0.09	0.17
0.10	0.08	0.15	0.21	0.16	0.08	0.10	0.06	0.08	0.12	0.13		

Table 8. The maximum annual flood discharges for the North Saskatchewan.

20.940	21.820	23.700	24.888	25.460	25.760	26.720	27.500	28.100
28.600	30.200	30.380	31.500	32.600	32.680	34.400	35.347	35.700
38.100	39.020	39.200	40.000	40.400	40.400	42.250	44.020	44.730
44.900	46.300	50.330	51.442	57.220	58.700	58.800	61.200	61.740
65.440	65.597	66.000	74.100	75.800	84.100	106.600	109.700	121.970

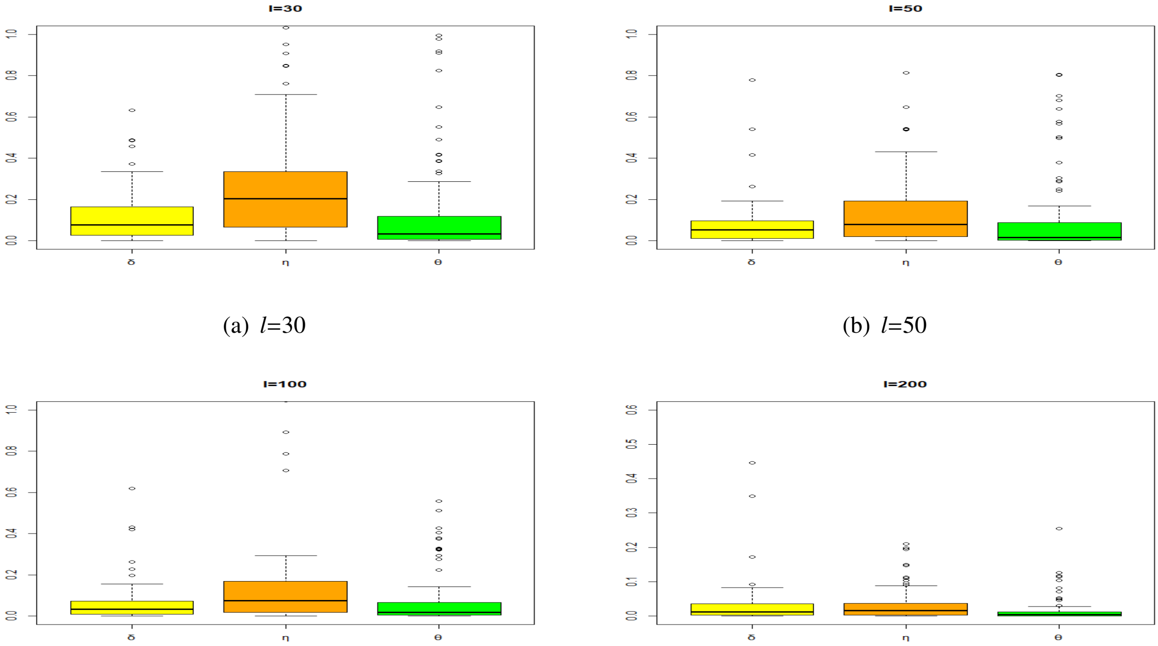

(a) l=30 (b) l=50

(c) l=100 (d) l=200

Figure 8. Box plots for the MSEs of of $\mathbf{\Delta} = (\delta, \eta, \theta)$ using set II.

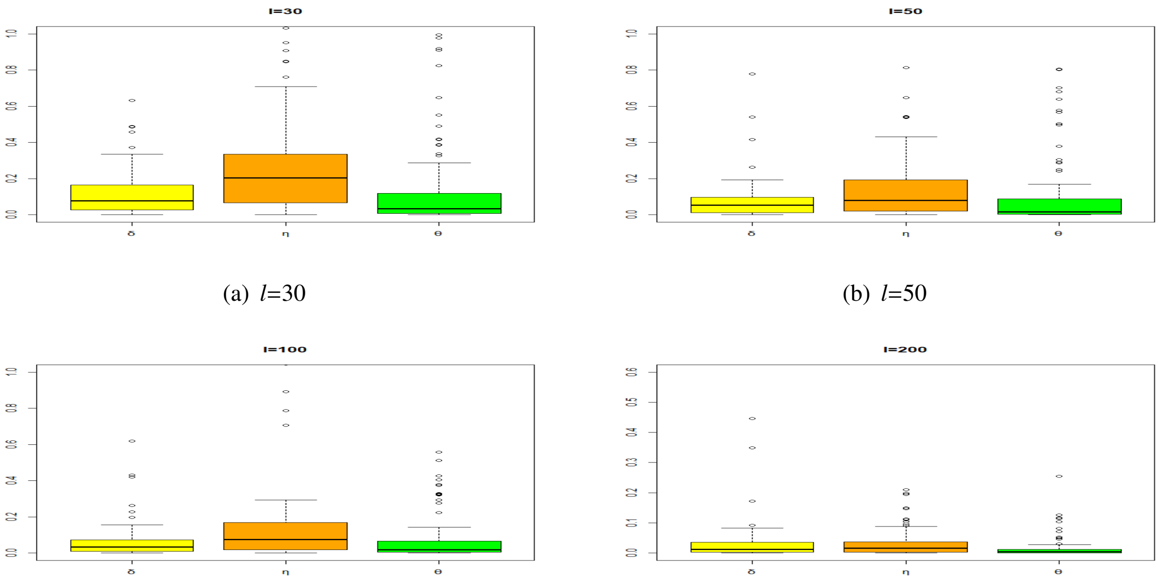

(a) l=30 (b) l=50

(c) l=100 (d) l=200

Figure 9. Box plots for the MSEs of of $\mathbf{\Delta} = (\delta, \eta, \theta)$ using set III.

recommended data sets. These plots further support the findings from Table (10), offering a very close fit to each data set as

Table 9. Summary Statistics of the two data sets.

n	Mean	Median	Q_1	Q_3	γ_3	γ_4
128	0.1408	0.1300	0.1000	0.1800	0.4490	-0.6814
45	47.65	40.40	30.38	58.80	1.3797	1.5138

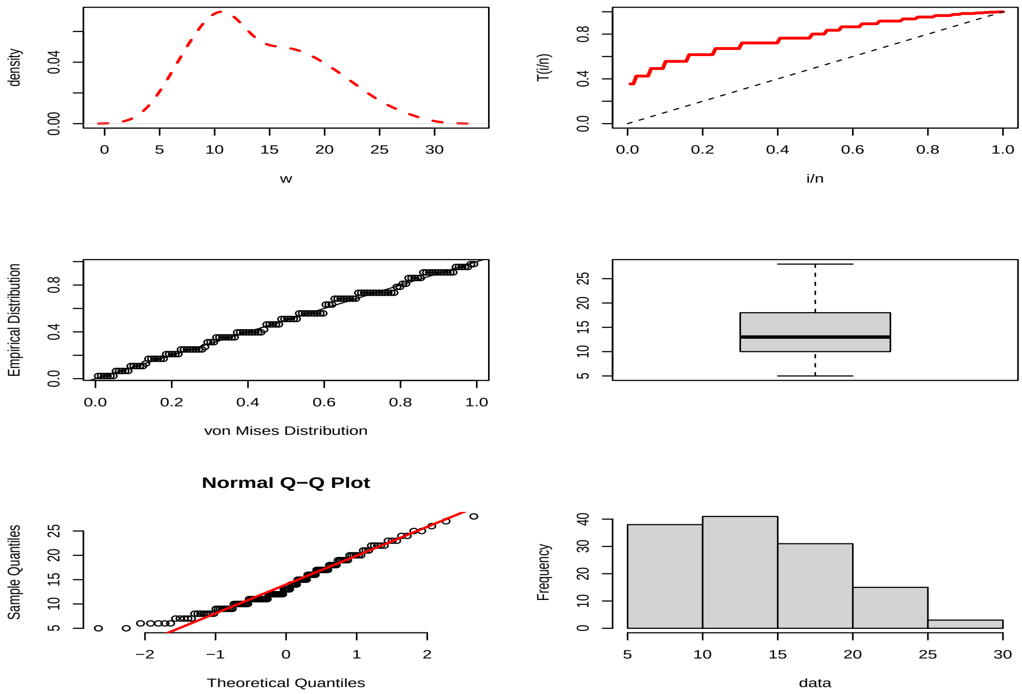

Figure 10. Several descriptive plots of data set I.

compared to the other contender distributions. Consequently, from the above comprehensive discussion, we can see that the newly proposed NOT-IRD is the best candidate for the considered data sets.

6. Concluding remarks

This study introduces a new flexible extension of the inverse Rayleigh distribution, called the new odd type-inverse Rayleigh distribution (NOT-IRD). The proposed distributions address a significant research gap in modeling complex statistical phenomena that traditional distributions may not adequately describe. The NOT-IRD can exhibit a variety of shapes, including skewed, decreasing, and unimodal patterns. We have derived various key theoretical characteristics of the NOT-IRD, including the quantile function, ordinary moments, and entropy information, along with the associated moment generating function. Based on the MLE method, we estimated the unknown parameters of the proposed model, and extensive simulation studies were conducted to evaluate the accuracy of the MLE technique. Additionally, we explore the practical applications of the NOT-IRD by modeling two real-life data sets. Based on our assessments, we observed that the NOT-IRD demonstrated improved goodness-of-fit and greater descriptive power compared to its traditional counterparts.

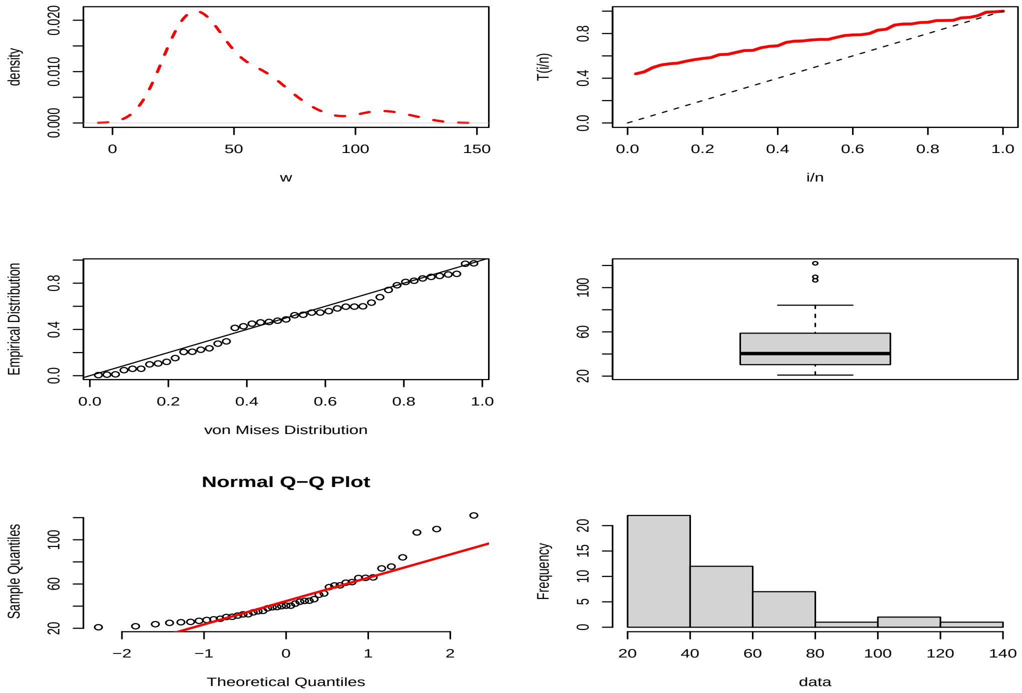

Figure 11. Several descriptive plots of data set II.

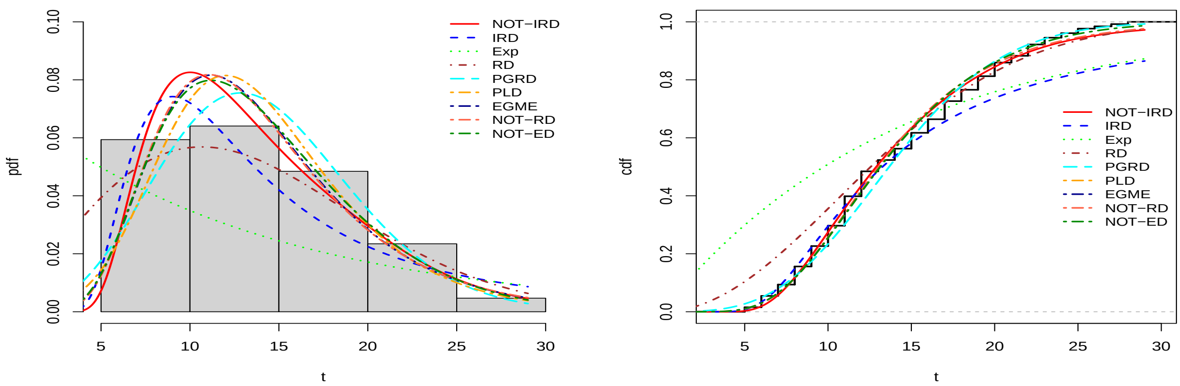

Figure 12. Estimation plots of pdf and cdf of the fitting distributions using data set I.

Authors' Contributions

All authors have worked equally to write and review the manuscript.

Data Availability Statement

All data are presented in the paper, along with their related references, in the Application section.

Table 10. Parameter estimators evaluate statistical metrics for the three accounting data sets.

Data	Model	$\hat{\delta}$	$\hat{\eta}$	$\hat{\theta}$	$\mathcal{AIC}$	$\mathcal{BIC}$	$\mathcal{KS}$	$\mathcal{P}$-value
	NOT-IRD	0.0369	0.0633	48.709	792.346	800.902	0.0705	0.5467
	NOT-ED	2.1443	14.584	0.2079	792.852	801.409	0.0798	0.3886
	NOT-RD	0.3380	4.4122	9.7332	792.495	801.052	0.0770	0.4325
	PGRD	12.177	0.0972	21.715	793.556	802.112	0.1099	0.0906
	EGME	0.0367	9.1771	0.1726	792.809	801.366	0.0796	0.3906
I	PLD		0.2824	7.5504	792.802	798.506	0.0892	0.2602
	IRD			11.047	822.204	825.056	0.1539	0.0046
	Exp			0.0710	935.023	937.875	0.3398	< 0.00001
	RD			10.667	812.788	815.640	0.15136	0.0056
	NOT-IRD	0.0415	32.180	26.168	396.289	401.709	0.0658	0.9898
	NOT-ED	0.2024	43.431	0.0569	397.477	402.897	0.0863	0.8904
	NOT-RD	0.3421	28.721	0.0564	397.627	403.047	0.0935	0.8263
	PGRD	47.009	0.0029	50.170	407.173	412.593	0.1482	0.2760
	EGME	0.0384	7.8345	0.6324	398.700	404.120	0.0983	0.7764
II	PLD		0.0815	5.7720	401.470	405.083	0.1144	0.5973
	IRD			36.631	397.304	399.111	0.1317	0.4152
	Exp			0.021	439.753	441.560	0.3558	< 0.00001
	RD			37.537	405.967	407.774	0.1440	0.3075

Conflicts of Interest

The authors declare no conflict of interest.

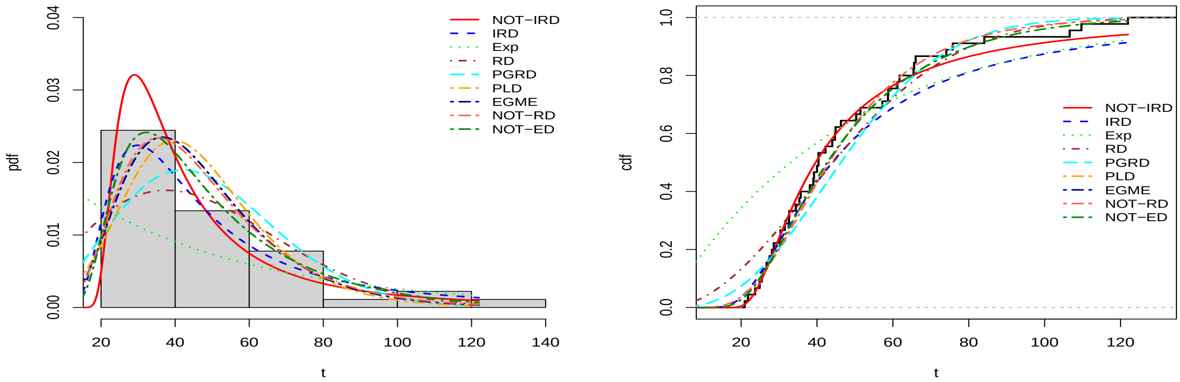

Figure 13. Estimation plots of pdf and cdf of the fitting distributions using data set II.

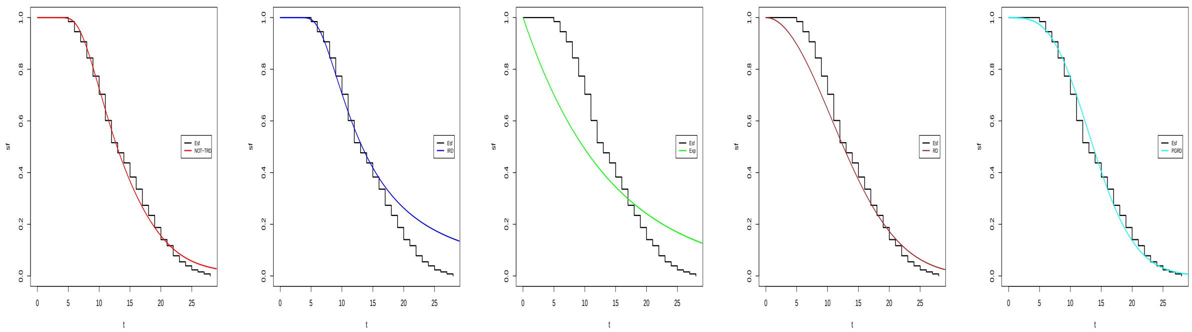

(a) NOT-IRD (b) IRD (c) Exp (d) RD (e) PGRD

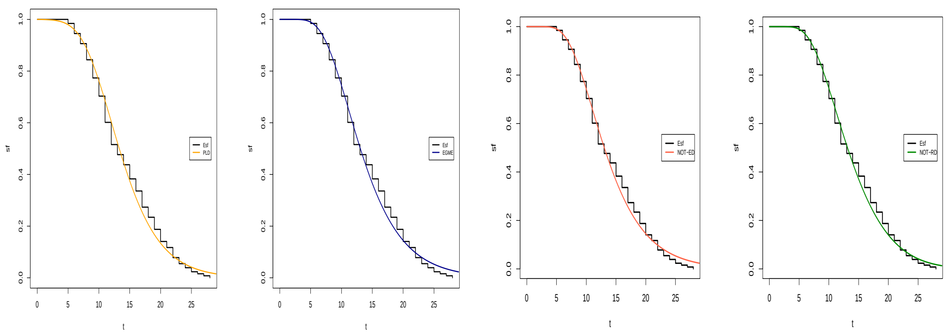

(f) PLD (g) EGME (h) NOT-ED (i) NOT-RD

Figure 14. Estimation plots of survival function of the fitting distributions using data set I.

Funding

There are no funds received for this paper.

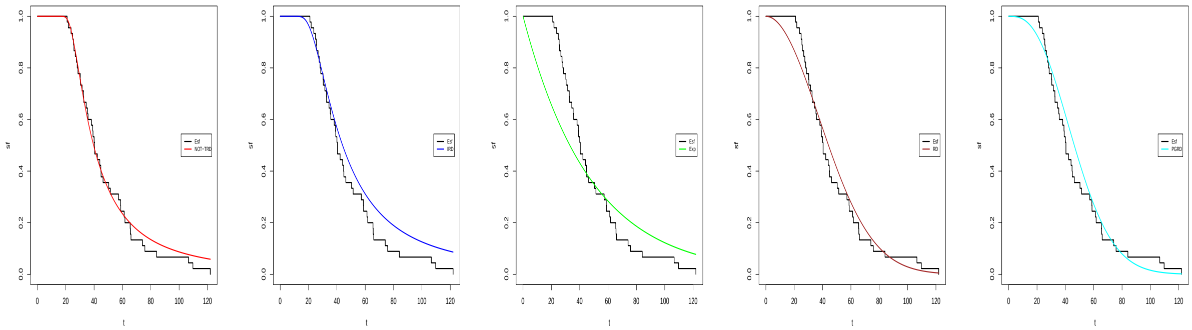

(a) NOT-IRD (b) IRD (c) Exp (d) RD (e) PGRD

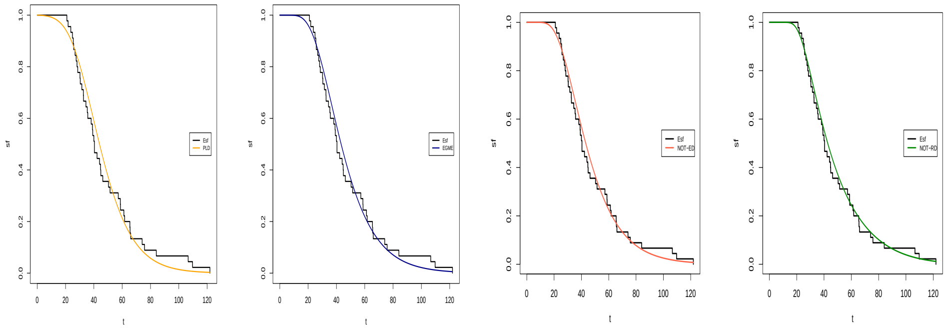

(f) PLD (g) EGME (h) NOT-ED (i) NOT-RD

Figure 15. Estimation plots of the survival function of the fitting distributions using data set II.

Use of Generative-AI tools declaration

The authors declare they have not used Artificial Intelligence (AI) tools in the creation of this article.

References

1. Mudholkar, G. S., Srivastava, D. K. (1993). Exponentiated Weibull family for analyzing bathtub failure-rate data, *IEEE Transactions on Reliability*, 42(2), 299-302.

2. Marshall, A.W., Olkin, I. (1997). A new method for adding a parameter to a family of distributions with application to the exponential and Weibull families, *Biometrika*, 84(3), 641-652.

3. Eugene, N., Lee, C., Famoye, F. (2022). eta-normal distribution and its applications, *Communication in statistics- theory and methods*, 31, 497-512,.

4. Shaw, W. T., Buckley, I. R. (2009). The alchemy of probability distributions: beyond Gram-Charlier expansions, and a skew-kurtotic-normal distribution from a rank transmutation map, *arXiv preprint arXiv*, 0901.0434.

5. Zografos, K., Balakrishnan, N. (2009). On families of beta- and generalized gamma-generated distributions and associated inference, *Statistical Methodology*, 6(4), 344–362.

6. Cordeiro, G. M., de Castro, M. (2011). A new family of generalized distributions, *Journal of Statistical Computation and Simulation*, 81(7), 883-898.

7. Alexander, C., Cordeiro, G. M., Ortega, E. M., Sarabia, J. M. (2012). Generalized beta-generated distributions, *Computational Statistics & Data Analysis*, 56(6), 1880-1897.

8. Alzaatreh, A, Lee, C, Famoye, F. (2013). A new method for generating families of distributions, *Metron*, 71, 63-79.

9. Bourguignon, M, Silva, R, Cordeiro, G. (2014). The Weibull- G Family of Probability Distributions, *J. Data Sci*, 12, 53–68.

10. Meraou, M.A., Al-Kandari, N., Raqab, M.Z., Kundu, D. (2021). Analysis of skewed data by using compound Poisson exponential distribution with applications to insurance claims, *Journal of Statistical Computation and Simulation*, 92(5), 928-956.

11. Meraou, M.A., Al-Kandari, N., Raqab, M.Z. (2022). Univariate and bivariate compound models based on random sum of variates with application to the insurance losses data. *Journal of Statistical Theory and Practice*, 16(4), 1–30.

12. Almetwally, E.M, and Meraou, M.A. (2022). Application of Environmental Data with New Extension of Nadarajah-Haghighi Distribution, *Computational Journal of Mathematical and Statistical Sciences*, 1(1), 26-41.

13. Mahdavi, A, and Kundu, D. (2017). A new method for generating distributions with an application to exponential distribution, *Communications in Statistics-Theory and Methods*, 46(13), 6543-6557.

14. Laxmi Prasad Sapkota, L.P., Nirajan, B., Kumar, V. (2024). A New Exponential Family of Distributions with Applications to Engineering and Medical Data, *arXiv preprint arXiv*, `doi.org/10.21203/rs.3.rs-4522315/v1`.

15. Smadi, M.M., Alrefaei, M.H. (2021) New extensions of Rayleigh distribution based on inverted-Weibull and Weibull distributions,*Int. J. Electr. Comput. Eng*, 11, 5107–5118.

16. Fatima, K., Ahmad, S.P. (2017). Weighted inverse Rayleigh distribution, Int. J. Stat. Syst, 12, 119–137.

17. Shala, M., Merovci, F. (2024). A New Three-Parameter Inverse Rayleigh Distribution: Simulation and Application to Real Data, *Symmetry*, 16, 634.

18. Mukherjee, S.P., Maiti, S.S. (1996). A percentile estimator of the inverse Rayleigh parameter, *IAPqR Trans*, 21, 63–66.

19. Soliman, A., Essam, A., Amin, A., Abd-El Aziz, A.A. (2010). Estimation and Prediction from Inverse Rayleigh Distribution Based on Lower Record Values, *Appl. Math. Sci*, 4, 3057–3066.

20. Rényi, A. On measures of entropy and information, *in Proc.4th Berkeley Symposium on Mathematical Statistics and Probability*, 547–561, University of California Press, 1960.

21. Shannon, C. A mathematical theory of communication, *Bell Syst. Tech. J*, 27, 379–423, 1948.

22. Tsallis, C. Possible generalization of Boltzmann-Gibbs statistics, *Journal of Statistical Physics*, 52(1-2), 479–487, 1988.

23. Oliveira, J., Santos, J., Xavier, C., Trindade, D., Cordeiro, C. (2013). The McDonald half-logistic distribution: Theory and practice, *Commun. Stat. Theory Meth*, 45(7), 2005-2022.

24. Van Montfort, M.A. (1970). On testing that the distribution of extremes is of type I when type II is the alternative, *J. Hydrol*, 11, 421–427.